Hyperfine-interaction parameters for a Cd probe atom at the Fe/Kr interface

P. Decoster, G. De Doncker, and M. Rots
Instituut voor Kern- en Stralingsfysika, Katholieke Universiteit Leuven, B-3030 Leuven (Heverlee), Belgium
(Received 15 September 1989)

Polycrystalline iron foils implanted to high krypton doses, in order to produce rare-gas inclusions, were doped with ^{111}In and the magnetic hyperfine field as well as the electric-field gradient was measured. Time-differential perturbed angular correlation experiments were performed in the as-implanted and the annealed sample condition. We observed a substantial fraction of probe atoms in a "defect site," characterized by the hyperfine interaction parameters $\Delta|B_{\rm hf}| = -6.89(4)\%$ and $V_{zz} \cong 2.6\times 10^{17}$ V/cm^2, in close similarity with those expected for the Kr/Fe interface. The impact of the present approach for metal surface studies is stressed.

I. INTRODUCTION

Recently, energy-band methods became increasingly powerful and reliable as a mathematical tool to study the electronic properties of condensed matter. Especially the application[1] of local-density-functional methods to the calculation of hyperfine fields in transition metals, molecular-cluster calculations[2] together with Green-function methods[3] for the impurity system, could explain the experimentally well-known hyperfine-field systematics to within almost 10%. For nonmagnetic *sp* impurities or magnetic $3d$ ($4d$)-probe impurities in transition metals, the dominant contribution to the hyperfine field $B_{\rm hf}$ arises from the Fermi contact interaction, thus the local magnetization density at the nucleus originating from the difference in majority and minority electron densities at the probe nucleus. The exchange interaction between host magnetic moments and the electron screening cloud around the impurity induces a critical balance between negative and positive contributions to the hyperfine field, largely determined by the impurity charge and the size of the impurity potential. The magnitude of the total hyperfine field apparently scales with the host magnetic moment, although this proportionality is not at all general, especially not in the case of the hyperfine field at metal surfaces. Indeed, while an experimental and theoretical consensus exists on the surface enhanced magnetization, recent Mössbauer work[4] on Fe(110) surfaces has shown that the hyperfine field at the Fe probe decreases. The predicted oscillatory behavior of the hyperfine field into the bulk region also contrasts with the absence of Friedel oscillations in the magnetic moment of the surface layers.[5] Furthermore, the important role of the broken symmetry at the surface reflects in the existence of a large electric-field gradient at the surface layer, not present beneath the top two layers.[6] From these observations one concludes that the contributions to the hyperfine field may significantly change, going from a surface to a bulk system. Essentially the modification of the negative valence contribution is supposed to be responsible for the observed effects strictly localized at the surface. This statement is particularly illustrated in the remarkable sensitivity of the "cleanness" of the surface, as has been noted in studies using overlayers.[7] There Friedel-type oscillations in the hyperfine field disappear near the Ag-coated surface and the field has the bulk behavior.

In addition to NMR and Mössbauer spectroscopy applied to the study of surface phenomena, perturbed angular correlation (PAC) techniques have been successfully applied (for a recent review see Ref. 8) in measurements of the electric-field gradient (EFG) for probe atoms at the surface of a nonmagnetic metal. Those experiments more than illustrate the power of PAC, and motivated a search for a complementary example in a magnetic system. The tremendous efforts needed to prepare clean surfaces and to deposit the hyperfine probe atoms on those surfaces, forced us to look for an alternative and more practical way to reach that goal. For this purpose we refer to recent investigations[9] dealing with the precipitation or bubble formation of rare gases in metals produced either by nuclear reaction or ion implantation. It is rather well established now,[10] that the bubbles are overpressurized and in solid phase, epitaxially aligned with the metal matrix. In the present paper, we report the first results on a search for hyperfine-interaction parameters for probes at the surface of a magnetic metal, by using the interface of a rare-gas inclusion in iron. In view of the general interest in surface physics as well as rare-gas precipitation, this approach may be most valuable.

II. EXPERIMENTAL DETAILS

A. Method

The method used is time-differential perturbed angular correlation (TDPAC), applied to the 175–247-keV γ-γ cascade in the decay of the nuclear probe ^{111}In to the nuclear ground state in ^{111}Cd. The electronic circuit is of the conventional fast-slow type,[11] with a time resolution typically 500 ps using BaF_2 detectors. The general expression for the angular correlation between two subsequent nuclear transitions in the decay is given by

$$W(\mathbf{R}_1,\mathbf{R}_2,t) = \sum_{\substack{k_1,k_2,\\ N_1,N_2}} A_{k_1}(1)A_{k_2}(2)G_{k_1k_2}^{N_1N_2}(t) \times [Y_{k_1}^{N_1}(\theta_1,\varphi_1)]^* Y_{k_2}^{N_2}(\theta_2,\varphi_2)\,. \quad (1)$$

The symbols have their usual meaning: (θ_i,φ_i) are the angles specifying the radiation directions R_i relative to a laboratory-frame z axis, the $A_{k_i}(i)$ coefficients are known radiation parameters, while $G_{k_1k_2}^{N_1N_2}(t)$ represents the perturbation factor describing the time dependent influence of extra nuclear (hyperfine-interaction) perturbation on the directional correlation of the radiations. The experiment is performed usually with four detectors placed at right angles in respect to each other. In order to eliminate the nuclear decay lifetime as well as efficiency differences between the detectors, a common practice is the evaluation of the so-called anisotropy factor

$$\mathcal{R}(t)=\frac{W_{ac}(\pi,t)W_{bd}(\pi,t)}{W_{ad}(\pi/2,t)W_{bc}(\pi/2,t)}-1\ , \tag{2}$$

the subscripts refer to each of the four detectors. Depending on whether or not the extra nuclear perturbation has a preferential spatial orientation, the $\mathcal{R}(t)$ factor differs. In the case of a randomly oriented magnetic interaction, we obtain

$$\mathcal{R}(t)=3A_{22}G_{22}(t)=\tfrac{3}{5}A_{22}[1+2\cos(\omega_B t)+2\cos(2\omega_B t)]\ , \tag{3}$$

neglecting orders higher than $k=2$. A similar expression for a randomly oriented electric quadrupole interaction reads

$$\mathcal{R}(t)=3A_{22}[0.2+0.371\cos(\omega_0 t)+0.285\cos(2\omega_0 t)+0.143\cos(3\omega_0 t)]\ . \tag{4}$$

The frequencies in those expressions represent the interaction strengths according to

$$\omega_B=\frac{g\mu_N B}{\hbar}\quad\text{or}\quad\omega_0=6\omega_Q=6\frac{eQV_{zz}}{\hbar 4I(2I-1)}\ . \tag{5}$$

In case the hyperfine interaction has a preferential orientation, the amplitudes of the frequency harmonics appearing in the Eqs. (3) or (4) become orientation dependent. For instance a magnetic interaction oriented perpendicular to the detector plane corresponds to an anisotropy factor $\mathcal{R}(t)$ containing, in Eq. (3) the second harmonic only. Finally, in most experiments the observed interaction frequency is not sharp, but distributed around some mean value with width δ. Therefore in the $\mathcal{R}(t)$ expression one should incorporate a multiplication factor $\exp(-n\delta\omega t)$ as an amplitude reduction for each nth frequency harmonic.

B. Sample preparation

A polycrystalline iron foil of high purity, preimplanted with krypton to a dose of 2×10^{16} ions/cm^2, was subsequently doped with ^{111}In (dose 4×10^{13} ions/cm^2) and post implanted with the same initial amount of krypton. The implantation energies were matched for an optimal depth profile overlap and the implantations were performed at room temperature. TDPAC experiments in the conventional four detector setup, were done on the samples as implanted as well as annealed for 30 min at temperatures up to 800 K. Along with zero-field measurements, we performed experiments in an external magnetic field, in the transversal and the longitudinal detector configuration, simultaneously. The latter geometry was intended to decouple partially the electric quadrupole interaction from the magnetic interaction, as will be explained later on.

III. RESULTS

A. Zero-external-field measurements

Earlier radiation-damage experiments on In-implanted pure iron,[12] have shown that low-temperature implantation at 80 K results in an almost 40% substitutional fraction corresponding to In probes at regular lattice sites in the Fe matrix. Implantation at room temperature, on the contrary, results in an almost nonexisting substitutional fraction and thus no well-defined spin precession pattern could be observed in the PAC spectrum. Furthermore, annealing above 473 K invokes a migration of indium probe atoms towards the surface and subsequent escape of the radioactivity.

In the present samples prepared at room temperature, however, already in the as-implanted condition an almost 50% indium fraction shows a precession pattern similar to a substitutional site occupation. This fraction is not essentially influenced by annealing. In Fig. 1 some results of the annealing sequence are displayed to illustrate this observation, all measurements were done at room temperature. Clearly the initial amplitude of the spin precession pattern remains essentially unchanged under isochronal annealing (30 min) at various temperatures up to 600 K. At higher anneal temperature, however, the indium probe becomes unstable and the precession frequency reduces to 30% of its unannealed value. Finally, at $T_A=773$ K the pattern completely disappears, suggesting that the indium probe experiences a broad distribution in interaction strength, before the activity escapes from the foil at $T_A=873$ K.

As a first approach to the analysis of those spectra, the data could be fitted reasonably well by an expression as Eq. (3) containing an unique probe site, characterized by an interaction frequency $\omega_B=555.8(1)$ Mrad/s and a width $\delta=6.8(2)$ Mrad/s. The observed fraction of indium probes in this hyperfine-interaction environment was 57% as implanted, increasing towards 70% after annealing at 373 K. No further change of fraction was seen until the anneal temperature $T_A=625$ K. The spectrum observed after $T_A=673$ K anneal corresponds with a broadly distributed hyperfine interaction with the parameters $\omega_B=175(2)$ Mrad/s and $\delta=21(2)$ Mrad/s. An improved fit to the data set could be obtained by assuming two probe sites for samples annealed below $T_A=600$ K. The first fraction of probe atoms experiences a well-defined interaction frequency of $\omega_B=555.3(2)$ Mrad/s and width $\delta=2.8(1.1)$ Mrad/s, while the other is somewhat ill defined with a broadened width. Obviously a combined magnetic and electric quadrupole interaction should be considered.

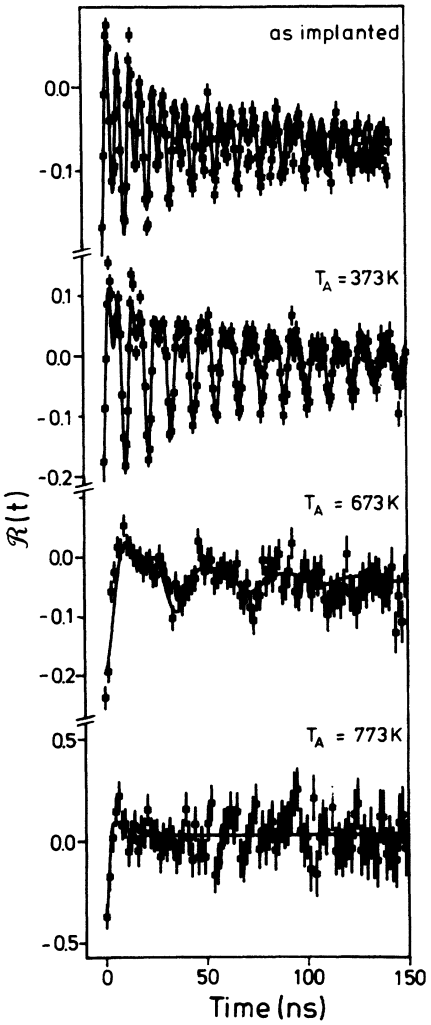

FIG. 1. Some TDPAC spectra measured at room temperature after different isochronal annealing steps.

B. External-field measurements

The sample of this experimental run is an iron foil (implanted as before) of dimensions $5\times15\times0.1$ mm^3 polarized in an external magnetic field of $|\mathbf{B}_{ext}|=0.1$ T, oriented perpendicular to the detector plane containing four detectors at 90° each. Those detectors were pairwise interconnected through the coincidence circuit in order to be used in the $\mathcal{R}(t)$ expression of Eq. (2). We call this detector configuration the *transversal geometry*. In addition another detector was placed along the $\mathbf{B}_{ext}$ direction, forming the "start" detector in the timing circuit, while the other four detectors were the "stop" detectors. The latter configuration will be called the *longitudinal geometry*. For this combination of the detectors the usual $\mathcal{R}(t)$ function can not be formed, because the PAC spectrum is measured at the inter detector angle 90° only. Therefore the data resulting from the longitudinal geometry will be analyzed directly according to the expression for the angular correlation given by Eq. (1).

Both geometries mentioned above were used *simultaneously* in an experiment on a sample annealed for 30 min at $T_A=373$ K and the result is shown in Fig. 2. The completely different shape of the PAC spectra for both geometries undoubtedly proves that i the probes experience a combined hyperfine interaction, ii the magnetic and the electric hyperfine interactions are not collinear. Indeed in a magnetized polycrystalline ferromagnetic foil the magnetic domains are aligned along the $\mathbf{B}_{ext}$ direction as is the hyperfine field $\mathbf{B}_{hf}$. In the longitudinal geometry the orientation axis of the nuclear spin alignment coincides with $\mathbf{B}_{ext}$ and therefore the Larmor precession does not change the angular correlation in case of a pure magnetic interaction. The same is true for a combined interaction with the magnetic and electric axes collinear, but not when the electric-field gradient (EFG) is uncorrelated with $\mathbf{B}_{ext}$ in orientation. When such a combined hyperfine interaction should be considered, the perturbation Hamiltonian is no longer diagonal with respect to a quantization axis along $\mathbf{B}_{ext}$ and therefore the angular correlation in longitudinal geometry not necessarily unperturbed. Referring to Eq. (1) one can show that in such a geometry no φ_2 dependence is expected, thus $N_2=0$, and moreover $N_1=0$ because of the choice of (θ_1,φ_1). The consequence is that only $k_1=k_2$ terms remain in Eq. (1). The shape of the longitudinal spectrum, however, will depend upon the relative strength of both the magnetic and electric interaction, i.e., the ratio $y=\omega_B/\omega_Q$.

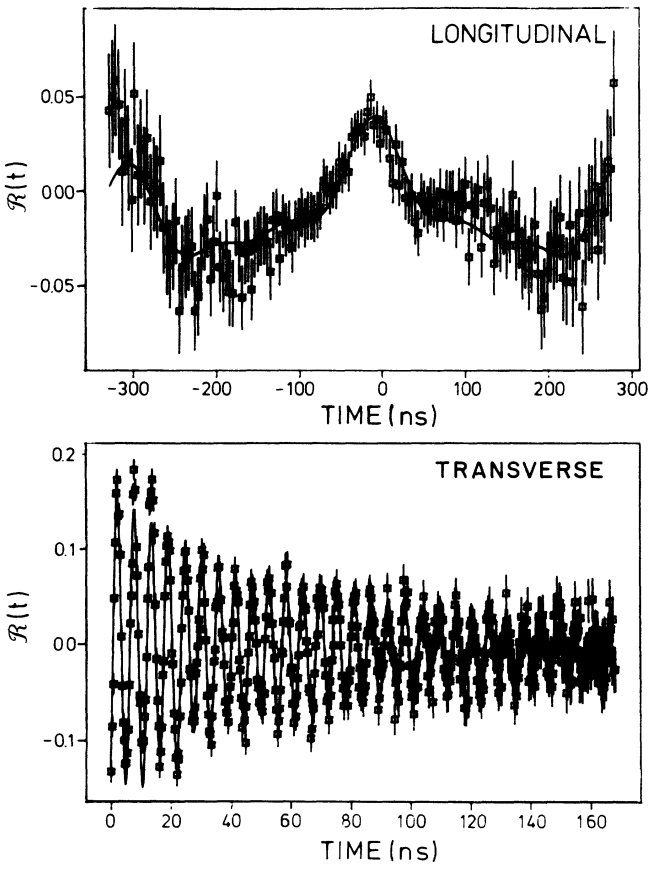

FIG. 2. Spin precession pattern for ^{111}Cd in Kr-implanted Fe measured in an external field of 0.1 T in transversal and longitudinal geometry, respectively.

In the extreme case of $y \ll 1$, we expect to observe the PAC spectrum shape corresponding to a randomly oriented electric quadrupole interaction and represented by Eq. (4). In the other extreme case, i.e., y large, we deal with an almost pure magnetic interaction, with its quantization axis along say detector one. As stated already, the angular correlation is unperturbed and thus constant in time. For intermediate cases the TDPAC spectrum evolves from almost constant towards a periodical pattern. More explicit discussion as well as some computer simulated spectra for a range of y values can be found in Ref. (13).

In Fig. 2(b) we see a spin precession, measured in *longitudinal* geometry. Note that those data were measured double sided in the time region $(-T, +T)$ and processed unfolded. As a first approach the precession pattern of Fig. 2(b) could be fitted with an expression similar to Eq. (4), but for two quadrupole sites with relative fraction $f_1 = 0.64$ and interaction frequency $\omega_{Q_1} = 3.53(5)$ Mrad/s, while $f_2 = 0.36$ with $\omega_{Q_2} = 1.1(1)$ Mrad/s for the second site. Moreover, the maximum observable correlation anisotropy is almost fully present, thus no unobserved fraction should be considered. The values for the EFG's corresponding to the observed interaction frequencies are, however, unreliable, because this analysis disregards the fact of a combined interaction. Nevertheless, no attempt to perform an exact analysis was undertaken, first because no analytical expression for such a case can be given[13] and moreover we only need to know the relative interaction strength y, approximately, to analyze the transversal spectrum. Therefore, we estimate from the longitudinal spectrum shape[13] that almost 40% of the probes are in an environment with a relatively small quadrupole interaction, the remaining fraction experiencing a combined interaction with $y \cong 1$, i.e., a rather strong quadrupole interaction.

The quadrupole interaction parameters, derived above from the longitudinal pattern, are a guide in the analysis of the data represented in Fig. 2(a), which correspond to a combined hyperfine interaction measured in *transverse* geometry. In such a geometry an almost pure magnetic interaction is reflected in a PAC pattern given by Eq. (3) with even frequency harmonics only because the sample is polarized perpendicular to the detector plane. The fraction of probes in an environment with a strongly combined interaction $y \cong 1$, on the contrary, will escape observation because of the incoherent superposition of a large number frequency components originating from the random orientation of the EFG in respect to $\mathbf{B}_{\rm hf}$. Therefore only some 40% (the f_2 fraction earlier) of the total correlation anisotropy will be present in the *transversal* spectrum and the PAC pattern contains *even* frequency harmonics of the magnetic interaction, shifted because of the presence of the quadrupole interaction. Because, for the fraction observed, the latter is small relative to the former, $\omega_Q/\omega_B \cong 6\times 10^{-3}$, in first-order approximation we expect frequency components of the type and close to

$$2\omega_B \pm 6\omega_Q\langle\beta\rangle \quad \text{and} \quad 2\omega_B \pm 18\omega_Q\langle\beta\rangle \ ,$$

with negligible contributions centered around ω_B. The factor $\langle\beta\rangle$ accounts for an averaging over the random orientation of the EFG relative to the external field direction.

In an analysis along those lines, the data from the transversal geometry could be fitted nicely when admitting more than one probe site, with the results being a "quasisubstitutional" site (fraction 40%) with $\omega_B = 554.7(1)$ Mrad/s, $\omega_Q = 0.42(14)$ Mrad/s, and $\delta = 9(1)$ Mrad/s; a "defect site" (fraction 15%) with $\omega_B = 520(2)$ Mrad/s, $\omega_Q\langle\beta\rangle = 2.7(2)$ Mrad/s, and $\delta = 10(5)$ Mrad/s; and an "undefined site" (fraction 10%) with $\omega_B = 130(2)$ Mrad/s and $\delta = 41(7)$ Mrad/s. The first two sites correspond to the f_2 fraction in the longitudinal spectrum. In addition almost 35% of the probes are unobserved, as mentioned before because of a combined interaction with comparable strengths, i.e., $y \cong 1$, such that the correlation anisotropy for that fraction dies out within the first nanoseconds of the measuring time. Those probes together with the "undefined site" fraction belong to the f_1 fraction mentioned earlier.

IV. INTERPRETATION

The results given explicitly in Sec. III B should be corrected for the external field. We obtain then for the quasisubstitutional site a hyperfine-field shift, relative to pure iron, of $\Delta|\mathbf{B}_{\rm hf}| = -6.8\times 10^{-3}$ and a mean value for the electric-field gradient (EFG) $\langle V_{zz}\rangle = [0.13(4)]\times 10^{17}$ V/cm^2. These hyperfine interaction parameters belong to probe atoms at regular iron lattice sites, the hyperfine field only slightly reduced because of the presence of krypton in the matrix, which also may be responsible for the small EFG. For the defect site, however, the hyperfine field shift equals $\Delta|\mathbf{B}_{\rm hf}| = -6.89(4)\%$ or -2.6 T, while $\langle V_{zz}\rangle = [0.86(6)\times 10^{17}]$ V/cm^2. Both of these values indicate that probes belonging to this fraction most probably experience fully the existence of krypton bubbles in the matrix. The quoted mean EFG value should be corrected for the random orientation. Because

$$\langle\beta\rangle \cong \langle P_2(\cos(\beta))\rangle = \tfrac{1}{3} \ ,$$

we estimate for the defect site $V_{zz} \cong 2.6\times 10^{17}$ V/cm^2. Finally, the undefined site most probably corresponds to probes in a damaged environment resulting from the ion implantation, because a similar site may be observed in pure iron also.

In what follows we would like to argue that the "defect site" can be identified as probes located at the interface of the krypton inclusion. The argument is as follows: As implanted condition: A remarkable high fraction of probes are implanted at well defined sites, where they experience a hyperfine field comparable with the one at substitutional sites in pure iron. This observation suggests that indeed Kr-bubble formation happens, thereby consuming the vacancies produced in the indium implantation. As a consequence only a minor fraction of probes, eventually those responsible for the undefined site will be associated with vacancy complexes because of radiation damage. Furthermore, Kr-decorated vacancy clusters around the In probe can eventually only explain the "unobserved" fraction, because the EFG value measured[14,15] for such configurations in cubic lattices is

indeed an order of magnitude larger than what we observed here for the "defect" site.

Quadrupole interaction strength: The value of the EFG at the "defect site" should be compared with the value (the EFG value has been corrected for the new quadrupole moment) $V_{zz}=8.10^{17}$ V/cm^2 observed at the Fe(110) surface in conversion-electron Mössbauer spectroscopy (CEMS) experiments.[4] Apparently our value for the EFG is substantially smaller compared with surface EFG values[8] not only for Fe but also for Cu. Note, however, that the value derived in the present experiment represents a mean value due to the random orientation, relative to the hfi axis, of the corresponding EFG. Moreover, we do not probe at a free surface and the Kr bubble (under high pressure[10]) may be of some importance in comparing EFG values.

Hyperfine-field shift: In the same CEMS experiment[4] one observes at clean Fe surfaces $\Delta|\mathbf{B}_{hf}|=-2.03$ T (first layer) and -0.11 T (second layer). The former value is in excellent agreement with the one observed here. Calculations of the magnetic hyperfine field[5] seems to predict substantial dependence on the symmetry of the surface. No characterization of the surface type, probed here at the Kr inclusion, was available as yet, and therefore quantitative comparison with theoretical estimates may be somewhat premature.

As a final remark we suggest that both fractions showing a well-defined precession in the TDPAC pattern (quasisubstitutional and defect site) eventually may be interpreted as originating both from the Fe/Kr interface, the latter at the surface the former in the outermost Fe layers. Indeed it is known from experiments[7] as well as recent EFG calculations,[16] that the cubic charge symmetry is restored some two layers beneath the metal surface.

V. CONCLUSION

With the present experiments we claim the first results on *impurity* hyperfine-field parameters at the *surface* of a *magnetic* metal matrix. We could determine a hyperfine-field reduction of 6.89(4)% relative to the pure iron bulk value, together with an electric-field gradient value similar to the one measured at nonmagnetic cubic metal surfaces. The present technique, when applied to an unpolarized sample, can not determine the symmetry of the surface itself but rather well the relative orientation of the surface EFG and the surface magnetization. Further work is in progress to derive this interesting correlation, which should allow the determination of the effective EFG value instead of an orientation average. Nevertheless, no essential influence on the hyperfine-field value and shift as quoted here may be expected from further work and present measurements are already conclusive on the hyperfine field. Let us stress that our results do not suffer from uncertainties due to residual gas adsorption, the main limitation in earlier work[7] on "quasiclean" surfaces. We therefore would like to conclude that our approach is promising as a complementary tool in the study of surface phenomena, however, without the need of expensive apparatus to produce and maintain clean surfaces. To perform the present studies, one only needs an ion implanter to create inert gas bubbles into the metal matrix and a probe with an affinity to occupy sites at the interface of those inclusions. The insolubility of indium in iron may well be responsible for the relatively large fraction of interface positions observed in the present experiment.

ACKNOWLEDGMENTS

The authors are indebted to Professor S. Bukshpan (Soreq, Israel) and Dr. H. Pattyn of the Instituut voor Kern- en Stralingsfysika (IKS, Leuven) for their proposal initiating the present study. This work was financially supported by the Belgian Interuniversitair Instituut voor Kernwetenschappen (IIKW).

[1]A. J. Freeman, J. Magn. Magn. Mater. **35**, 31 (1983).
[2]B. Lindgren and D. E. Ellis, Phys. Rev. B **26**, 636 (1982).
[3]S. Blugel, H. Akai, R. Zeller, and P. H. Dederichs, Phys. Rev. B **35**, 3271 (1987).
[4]M. Przybylski and U. Gradmann, Phys. Rev. Lett. **59**, 1152 (1987).
[5]S. Ohnishi, M. Weinert, and A. J. Freeman, Phys. Rev. B **30**, 36 (1984).
[6]J. Koréchi and U. Gradmann, Phys. Rev. Lett. **55**, 2491 (1985).
[7]J. Koréchi, Hyp. Int. **40**, 89 (1988), and references therein.
[8]G. Schatz, R. Fink, T. Klas, G. Krausch, R. Platzer, J. Voigt, and R. Wesche, Hyp. Int. **49**, 395 (1988).
[9]A. vom Felde, J. Fink, Th. Muller-Heinzerling, J. Pfluger, B. Scheerer, and G. Linker, Phys. Rev. Lett. **53**, 922 (1984).
[10]H. H. Andersen, J. Bohr, A. Johansen, E. Johnson, L. Sarholt-Kristensen, and V. Surganov, Phys. Rev. Lett. **59**, 1589 (1987).
[11]A. R. Arends, C. Hohenemser, F. Pleiter, H. de Waard, L. Chow, and R. M. Suter, Hyp. Int. **8**, 191 (1980).
[12]F. Pleiter, C. Hohenemser, and A. R. Arends, Hyp. Int. **10**, 691 (1981).
[13]F. Pleiter, A. R. Arends, and H. G. Devare, Hyp. Int. **3**, 87 (1977).
[14]M. Deicher, G. Grubel, W. Reiner, and Th. Wichert, Hyp. Int. **15/16**, 467 (1983).
[15]R. Vianden, in *Nuclear Physics Applications on Materials Science,* Vol. 144 of *Nato Advanced Study Institute, Series E: Applied Sciences,* edited by E. Recknagel and J. C. Soares (Kluwer, London, 1988), p. 239.
[16]B. Lindgren, Hyp. Int. **34**, 217 (1987).